Hindawi
Journal of Sensors
Volume 2020, Article ID 1571936, 11 pages
https://doi.org/10.1155/2020/1571936

Research Article

Wheat Grain Yield Estimation Based on Image Morphological Properties and Wheat Biomass

Tchalla Korohou,[1] Cedric Okinda,[1] Haikang Li,[1] Yifei Cao,[1] Innocent Nyalala,[1] Lianfei Huo,[1] Mouloumdèma Potcho,[2] Xiang Li,[1] and Qishuo Ding[1]

[1]*College of Engineering, Nanjing Agricultural University/Key Laboratory of Intelligent Agricultural Equipment of Jiangsu Province, Nanjing 210031, China*
[2]*College of Agriculture, South China Agricultural University, Guangzhou 510642, China*

Correspondence should be addressed to Qishuo Ding; qsding@njau.edu.cn

Received 15 October 2019; Revised 17 March 2020; Accepted 25 May 2020; Published 12 September 2020

Academic Editor: Heinz C. Neitzert

Copyright © 2020 Tchalla Korohou et al. This is an open access article distributed under the Creative Commons Attribution License, which permits unrestricted use, distribution, and reproduction in any medium, provided the original work is properly cited.

The estimation of wheat grain yield based on a composite of morphological features and mass of wheat organs was introduced in this study. The morphological features (length, width, and perimeter for the wheat stem and ear) were extracted by a computer vision system whose performance was evaluated by correlating the measured and estimated perimeter and length of the wheat stem at an R^2 of 0.9609 and 0.9779, respectively. Six regression models were developed based on the extracted features. The linear regression based on the wet weight of the stem, the ear, and the leaves outperformed all the other statistical models explored with an R^2 of 0.9893 and an RMSE of 0.0684 mm in estimating the dry grain yield with wet wheat organ mass as the predictors. This proposed system can be applied as nondestructive in a field technique for wheat phenotyping. Additionally, it can be applied to other similar crops.

1. Introduction

Food security concerns have mandated an increase in agricultural production due to the ever-growing world population with a projection of over 9.6 billion people by the year 2050 [1]. However, environmental production constraints have resulted in a decline in the global per capita cereal production since the early 1980s. Hence, the global population growth rate has surpassed the cereal production [2]. Therefore, a new green revolution is needed to solve the impending global food security problem by improving the productivity of all major food and energy crops [3]. Improved productivity in crop production can only result from increased genetic gains. Hence, current crop breeding strategies must be improved [4]. Plant genetics have a high potential in the revolution of plant breeding techniques by characterizing the genetic material and allowing the identification of loci and the manipulation of genes of interest to make a dynamic selection for crop improvements [5, 6].

Genomic selection requires accurate high-throughput field phenotyping techniques. However, conventional plant breeding is a bottleneck to high-throughput field phenotyping [7, 8]. Over the past three decades, the genomic revolution and advances in technology have resulted in significant improvements in genomic information acquisition [9]. These technologies are based on phenotyping by the use of imagery for noninvasive analysis of the structural and physiological traits related to plant performance [10]. Due to its perceived importance, intensive research efforts are currently underway on automated high-throughput phenotyping of plants [9].

This study is based on the wheat plant because it is an important global food crop [11]. Hence, an improvement in its production will help alleviate global food security problems. Several studies have established that biomass and morphological parameters of various organs of wheat shoots are essential references for phenotyping crop growth and yield formation [12]. Watanabe et al. [13] and Hu et al.

[14] reported that the height of a wheat plant is a significant indicator of the morphological parameters of the phenotype of a crop, which can directly reflect the growth status of the crop and is closely related to yield. Additionally, the ear and the ear edge features are vital parameters that directly reflect the growth of wheat [15]. As a result, several experimental field-based phenotyping platforms have recently been developed to study these different traits (height, ear, and their morphology features) in relation to the physiological performance of the plant. These platforms vary in mechanical design, sensors, data communication, and acquisition systems. Mechanical designs ranged from handcars to towed trailers, from self-propelled vehicles to robots [16]. Different techniques to measure spectral characteristics of the wheat canopy, height, and vegetation cover characteristics (vegetation index and the texture of the canopy) have also been introduced [17]. Additionally, Hosoi and Omasa [18] using a LIDAR scanner for canopy profiling of wheat voxel estimated the vertical canopy density profiles of wheat at different growth stages (tillering, stem elongation, flowering, and maturation).

The conventional method of counting wheat ears is performed manually. However, this technique is subjective, inaccurate, and time consuming [19]. With the current development in information technology, several vision-based systems have been introduced in wheat phenotyping [20, 21]. All the techniques developed for plant phenotyping open up the possibility of forming plant models with a high level of detail. However, to reduce outlays, the possibilities of using a single camera without other additional equipment remain a challenging task. The development of image acquisition algorithms and the quality of models must be explored.

Plant phenotyping allows researchers to gather information that is useful for assessing growth, physiology, architecture, stress, yield, and each development of the plant, thereby enabling more complete management of the plant [22]. However, the vegetal improvement of wheat must go through the identification of phenotypes that are likely to influence the final grain yield directly. It will, therefore, be necessary to establish the relationship between each phenotype, first taken individually and then taken together, and the final grain yield. However, in most studies, the phenotypic index is based on a single wheat organ such as the height [14], the number of tillers [19], the number of ears [15], and the reflectance of the canopy [18] using image processing technology and has not established the relationship between the different phenotypes and the final grain yield.

In the context of nondestructive measurement of crop growth, Li et al. [22] pointed out that the stem and leaf indicators can provide more information about plant growth. Kun et al. [15] reported that the precision of identification in the morphological characteristics and classification of wheat ears could be improved if the indexing parameters of the stems and wheat leaves are combined. Furthermore, in the context of research on wheat growing techniques, Yu et al. [23] pointed out that more attention should be given to the overall performance of the stem and leaf and ear traits. However, the mentioned studies failed to take into account both the morphological parameters of the ear and the stem to accurately reflect the growth state of the wheat, which could be a reference for the rapid classification of wheat species. Therefore, the use of composite phenotypic wheat indicators to reflect crop growth and the final crop yield analysis is a significant means of optimizing the quality of the wheat plant density which often results in nonuniformities during individual growth and development [24].

As much as the previous studies have been performed on yield estimation, the ear morphology should be considered a factor affecting yield. Therefore, this study applied composite phenotype indicators (leaves, stem, and ear) to estimate the wheat grain yield. The main objective of this study was to estimate the wheat grain yield based on wheat organ weight and morphological parameters (length, width, surface area, and perimeter). The specific objectives were (1) to develop an efficient image processing technique to perform morphological feature extraction and (2) to develop regression models to estimate the weight yield based on the extracted feature variables.

2. Materials and Methods

2.1. Description of the Site. This study was conducted in Nanjing Agricultural University, Jiangsu Experimental Farm, Babaiqiao, Luhe, Jiangsu, China. The site was located at 31°98′N, 118°59′E in a subtropical monsoon climate, with an annual rainfall of approximately 1000 mm and an average temperature of 15.8°C [25]. Rice-wheat rotation is a long-established agricultural system in this region. Characterized by a paddy season between June and late November. One month before rice harvest, the field was drained to allow the soil to dry out for mechanical harvesting, after which the subsequent crop season, i.e., wheat or canola, is ensued [26]. Soil organic matter, total nitrogen, available nitrogen, available phosphate, and available potassium were estimated at $8.24\,g\,kg^{-1}$, $0.97\,g\,kg^{-1}$, $12\,mg\,kg^{-1}$, $12.67\,mg\,kg^{-1}$, and $11.05\,mg\,kg^{-1}$, respectively. The pH, bulk density, and soil moisture content were established to be 7.6, $1.26\,gcm^{-3}$, and 29.3%, respectively, according to the study by Lu [27].

2.2. Crop Husbandry and Experimental Design. A one-year field experiment was conducted during the 2017 wheat season, in which, two wheat varieties, "Luyuan 502" (V502) and "Zhengmai 9023" (V9023), were sowed in this study. Direct seeding, a typical conservation agriculture system [28], was adopted and carried out manually on 6th November 2017 on no-till soil with an interrow distance of 20 cm at approximately 1.5 cm between the seeds. Phosphate, urea, and potassium chloride were applied on the soil surface at $120\,kg\,hm^{-2}$,$150\,kg\,hm^{-2}$, and $135\,kg\,hm^{-2}$, respectively [25]. The whole wheat season was rain fed, and harvesting was performed manually and retrieved back to the laboratory. A summary of the entire experiment design is shown in Figure 1.

2.3. Image Acquisition System and Sample Preparation. The 50 heads of each wheat variety were sampled from the field using a random sampling technique [29] similar to the study by Yates and Zacopanay [30]. Therefore, the selected 50

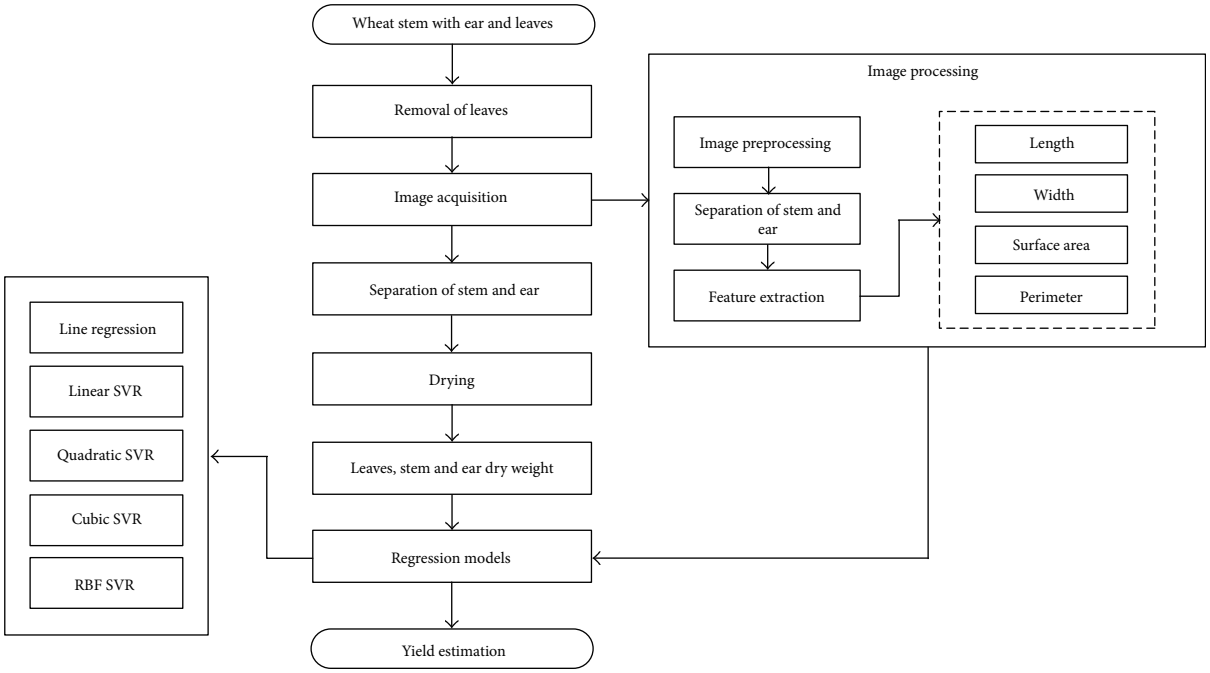

Figure 1: Flow chart of the entire experimental design.

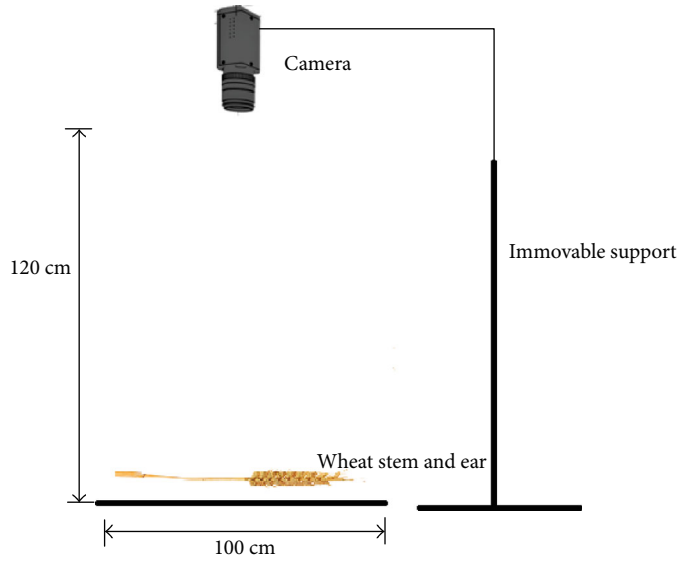

Figure 2: Experiment setup and Image acquisition.

heads of each wheat variety sample were a representation of the wheat population in the field. Since mature wheat's leaves are yellow, it is difficult to extract the true parameters of leaf morphology by image processing [9]. Hence, this study was based on the morphological parameters of the stem and ear. For each stem, leaves were manually removed using a pair of scissors and kept for further processing (wet and dry weight extractions). The stems without the leaves were placed on a white background plate to obtain diffuse illumination of the canopy during image acquisition [31]. Wheat stem and ear images were captured using Nikon D3200 digital camera (1920 by 1080 pixels) mounted 120 cm vertically above the center of the imaging platform, as shown in Figure 2. The camera was prior calibrated by the checkerboard camera calibration technique [32] such that 1 pixel equals to 1 mm.

Crop research and model development requires a large number of data samples. Therefore, during image acquisition, each stem was rotated by 120° with the longitudinal length as the axis of rotation. Thus, for each wheat head, 30 images were acquired, 10 for each orientation.

Several single-stem ear combinations were taken in a single image to save test time, after which every single stem was extracted during the morphological parameter feature

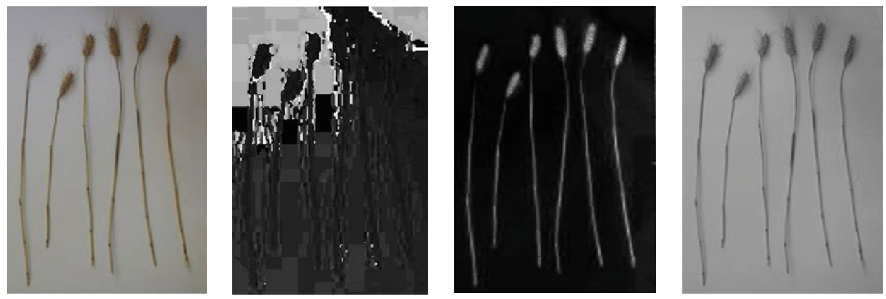

(a) (b) (c) (d)

Figure 3: Image conversion from RGB to HSV color space. (a) Original image RGB color space. (b) H-space image. (c) S-space image. (d) V-space image.

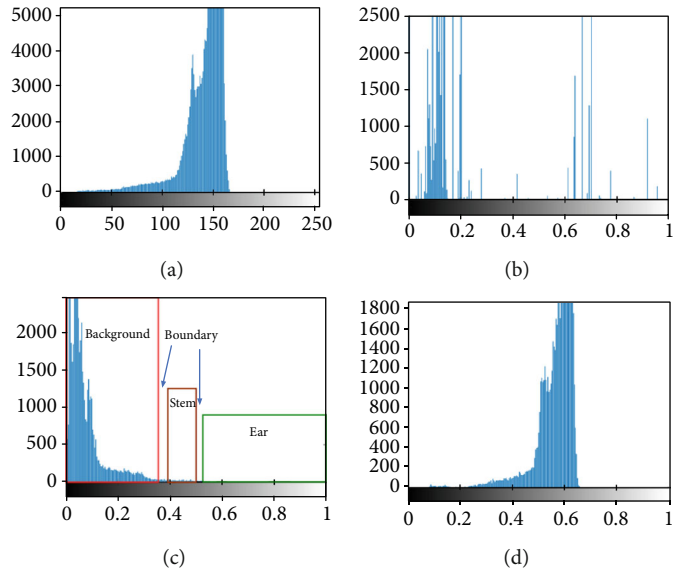

Figure 4: (a) Histogram of the pixel values of the RGB color space image. (b) Histogram of the pixel values of the H-space image. (c) Histogram of the pixel values of the S-space image showing the segmentation region of the ear and the stem. (d) Histogram of the pixel values of the V-space image.

extraction process. The acquired images were transferred to a personal computer for further processing.

On completion of image acquisition, the leaves, stem, and ear of each wheat plant sample were placed in separate plastic fillet bags to prevent sample mixing. The leaves, stems, and ears were dried at 105°C using an electric blast drying box (Model HG 01-2A, Nanjing Honglong Instrument Equipment Factory) for 24 hrs to a constant weight. Finally, the individual weight of each organ was recorded per wheat sample [33]. Dried wheat ears were subjected to a threshing treatment using a single-ear thresher (Model Ki-100, Changzhou Dedu Precision Instrument Co., Ltd., factory) to obtain a single-eared yield.

2.4. Image Processing. In any image processing operation, image preprocessing and segmentation techniques greatly influence the accuracy of the system being developed [34]. Preprocessing is often applied to remove the background and noise due to variations in the ambient light conditions. The following image preprocessing procedure was applied.

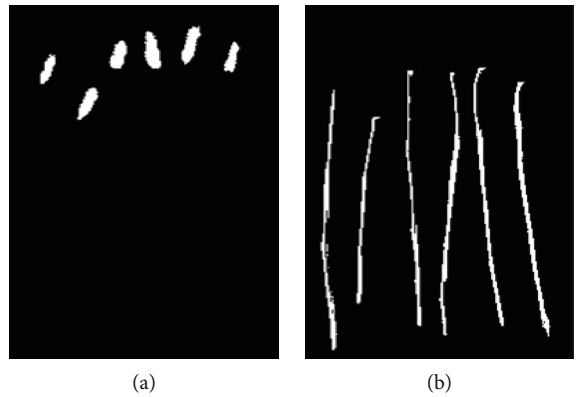

(a) (b)

Figure 5: (a) Segmentation of the ear. (a) Segmentation of the stem.

Step 1. The color index of vegetation extraction (CIVE) was performed on the images according to Equation (1) [19, 35, 36]. Since the image acquisition was performed under natural light, the images were subjected to external interference and poor illumination uniformity.

Table 1: A description of the feature variables.

Organ	Features	Description
Stem	Length (l_s)	Distance from the bottom of the stem to the ear section
	Width (W_s)	The width of the stem
	Surface area (A_s)	Number of pixels occupying the image of the stem
	Perimeter (P_s)	Number of pixels around the boundary of the image of the stem
Ear	Length (l_e)	The length of the spike to the end of the ear
	Width (W_e)	Width of the ear
	Surface area (A_e)	Number of pixels occupying the image of the ear of wheat
	Perimeter (P_e)	Number of pixels around the boundary of the image of the ear
Wet weight	Leaf (L_w)	Weight of the fresh leaves
	Stem (S_w)	Weight of the fresh stem
	Ear (E_w)	Weight of the fresh ear
Dry weight	Leaf (L_d)	Weight of the leaves after drying treatment
	Stem (S_d)	Weight of the stem after drying treatment
	Ear (E_d)	Weight of the ear after drying treatment

$$\mathrm{CIVE} = (0.441\mathrm{R} + 0.811\mathrm{G} + 0.385\mathrm{B} + 18.7874) \quad (1)$$

where R, G, and B are the red, green, and blue color spaces.

Step 2. Gaussian filter was applied to the image by Equation (2) to remove noise [37]. Because the background was white with low saturation, the partial saturation of the stems was much higher than that of the background.

$$\mathrm{G}(\mathrm{x}, \mathrm{y}) = \frac{1}{2\pi\sigma^2} \mathrm{e}^{-\left(\mathrm{x}^2+\mathrm{y}^2\right)/2\sigma^2} \quad (2)$$

where σ is the standard deviation of the distribution. The distribution was assumed to have a mean of 0.

Step 3. To segment the ear and the stem, the images were then transformed from the RGB color space to HSV color space, as shown in Figure 3.

Step 4. The S space was selected for histogram analysis to determine the threshold values for each organ [38], as shown in Figure 4(c). Furthermore, from Figure 3, the S space showed more distinctive values for each organ compared to the H and V spaces. Therefore, to segment the ear and the stem, threshold values obtained from the S space were applied according to Equations (3) and (4) for ear and stem segmentation, respectively.

$$\mathrm{Ie}_{x,y} = \begin{cases} 1, & \text{if } \mathrm{Io}_{x,y} \geq \mathrm{Te}, \\ 0, & \text{otherwise}, \end{cases} \quad (3)$$

$$\mathrm{Is}_{x,y} = \begin{cases} 1, & \text{if } \mathrm{Ts}_{\min} \leq \mathrm{Io}_{x,y} \leq \mathrm{Ts}_{\max}, \\ 0, & \text{otherwise}, \end{cases} \quad (4)$$

Table 2: The properties of the models developed.

Models	Feature variables used to estimate dry yield
Mdl1	L_w, S_w, and E_w
Mdl2	L_d, S_d, and E_d
Mdl3	l_s, W_s, A_s, P_s, l_e, W_e, A_e, and P_e
Mdl4	l_s, W_s, A_s, and P_s
Mdl5	l_e, W_e, A_e, and P_e
Mdl6	L_d, S_d, E_d, l_s, W_s, A_s, P_s, l_e, W_e, A_e, and P_e

where $Ie_{x,y}$ and $\mathrm{Is}_{x,y}$ are the binary images of the ear and the stem, respectively; $Io_{x,y}$ is the original image in the S space of HSV; Te is the threshold value of image intensity for segmentation of the ear, $Ts_{\min}$ and $Ts_{\max}$ are the minimum and maximum threshold values for the segmentation of the stem. Figure 5 presents the segmented wheat stem and ear.

Step 5. Performed morphological opening of the resultant binary images by a disk structural element of size 5×9 pixels to remove small holes to obtain a clear binary image.

2.5. Feature Extraction. Morphology is one of the most effective features useful in discriminating objects in the crop phenotyping as it describes an object with respect to shape and visual characteristics [39]. Therefore, a comparison of two wheat cultivars was carried out based on the morphological parameters. Using the image processing toolbox of MATLAB software, four morphological features were extracted for each ear and stem [15]. A description of all the extracted feature variables in this study is shown in Table 1.

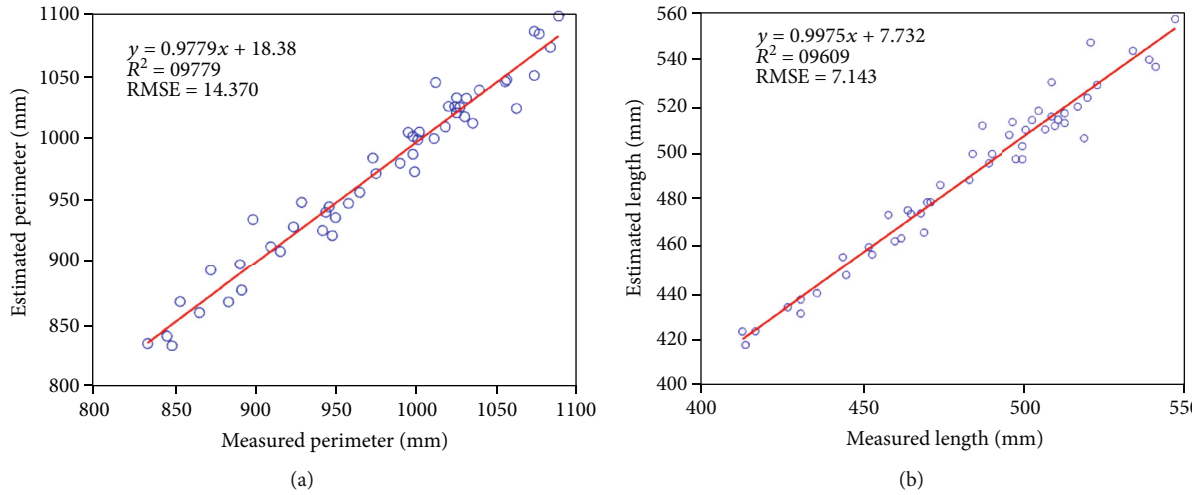

Figure 6: Scatter plot of the relationship between the perimeter and length measured and estimated (a) stem perimeter and (b) stem length.

Table 3: Comparison between measured and estimated stem length (mm).

Measured	Estimated	Error	Relative error
513	516.822	3.822	0.745
501	509.728	8.728	1.742
503	513.955	10.954	2.178
523	529.044	6.044	1.156
509	515.488	6.488	1.275
470	478.556	8.556	1.820
498	497.205	-0.795	0.160
497	513.102	16.102	3.240
445	447.208	2.208	0.496
474	486.027	12.026	2.537

Average relative error ($n = 50$) =1.554%.

Table 4: Comparison between measured and estimated stem perimeter (mm).

Measured	Estimated	Error	Relative error
1032	1033.056	1.056	0.102
1019	1009.845	-9.155	0.898
1036	1012.720	-23.280	2.247
1074	1051.417	-22.583	2.102
1028	1025.727	-2.273	0.221
930	949.058	19.058	2.049
999	1002.162	3.162	0.317
1012	1000.284	-11.716	1.158
892	898.419	6.419	0.720
1032	1033.056	1.056	0.102

Average relative error ($n = 50$) =1.174%.

2.6. Regression Models. To predict the wheat grain yield based on the extracted feature variables, five regression models were explored in this study, namely, support vector regression (SVR) models (linear, quadratic, cubic, and radial basis function (RBF)) and linear regression. Introduced by Boser et al. [40], SVR is a regression solver of support vector machines (SVMs), it does not require a large number of training samples with impressive generalization performance [41, 42], which provides direct geometric interpretation and avoids overexploitation of data [43]. For more information on SVR, please refer to the studies of Wu and Zhou [44]. For dry grain yield prediction, six models were developed as described in Table 2. The dataset included 1500 samples. The dataset was divided into a training set of 1050 samples (70%) and a test and validation set of 450 samples (30%).

Table 5: Descriptive statistics for the dry wheat grain yield measured of both varieties ($n = 50$).

Descriptive statistics	V502 value (g)	V9023 value (g)
Mean	1.019	1.060
Standard error	0.057	0.067
Median	0.949	1.113
Mode	0.762	0.784
Standard deviation	0.403	0.477
Sample variance	0.1632	0.228
Skewness	1.225	0.729
Range	2.335	2.245
Minimum	0.178	0.253
Maximum	2.513	2.498

2.7. Statistical Analysis. A descriptive analysis was performed on the measured wheat grain yield for both varieties ($n = 50$). The statistical analyses were performed using the analysis option in Microsoft Excel 2019 (Ms corporation, Redmond, WA). Also, to verify the accuracy of the image processing, the relationship between the measured and the estimated stem length and stem perimeter were analyzed by linear an adjustment technique using the Curve Fitting Toolbox in MATLAB R2019a software (The Mathworks Inc., Natick, MA, USA).

Table 6: Performance evaluation of the six models used for wheat grain yield estimation.

Regression models	Mdl1		Mdl2		Mdl3		Mdl4		Mdl5		Mdl6	
	V502	V9023	V502	V9023	V502	V9023	V502	V9023	V502	V9023	V502	V9023
Linear regression	0.9893	0.9869	0.986	0.987	0.9563	0.880	0.8981	0.8667	0.9665	0.844	0.956	0.8809
Linear SVR	0.9757	0.9568	0.967	0.956	0.9525	0.930	0.8981	0.9319	0.9653	0.8767	0.9652	0.9489
Quadratic SVR	0.9762	0.9573	0.967	0.957	0.9532	0.931	0.8993	0.9318	0.9655	0.9032	0.9650	0.9492
Cubic SVR	0.9833	0.8646	0.885	0.986	0.1197	0.063	0.8868	0.7215	0.9588	0.8967	0.9598	0.2454
RBF SVR	0.9735	0.9539	0.964	0.953	0.9504	0.928	0.8947	0.9299	0.9633	0.8731	0.9633	0.9469

V502 = "Luyuan 502" and V9023 = "Zhengmai 9023".

Table 7: The summary of performance evaluation of the best linear regression, linear, and quadratic SVM model, where SSE is the square sum error of the estimate, R^2 is the coefficient of determination, R^2 adj. is R-squared adjusted for the degree of freedom, and RMSE.

	Mdl1		Mdl2		Mdl3		Mdl4		Mdl5		Mdl6	
	V502	V9023	V502	V9023	V502	V9023	V502	V9023	V502	V9023	V502	V9023
SSE	2.096	2.311	2.035	2.184	8.137	10.07	15.55	9.841	6.333	14.46	5.326	7.405
R^2	0.9893	0.9869	0.986	0.987	0.9563	0.931	0.8993	0.9319	0.9665	0.9032	0.9652	0.9492
R^2 adj	0.9892	0.9869	0.986	0.987	0.9562	0.9309	0.8991	0.9317	0.9664	0.9032	0.9651	0.9491
RMSE	0.0684	0.0718	0.0764	0.1204	0.1348	0.1499	0.1863	0.1482	0.1189	0.1796	0.1092	0.1286

V502 = "Luyuan 502" and V9023 = "Zhengmai 9023".

3. Results and Discussions

3.1. Image Processing Evaluation. In order to evaluate the performance of the image processing algorithm, the relationship between the perimeter and the length of the stem for manually measured and estimated values (by image processing) on a selected set of 50 stems for variety V502 was explored in terms of accuracy.

Figures 6(a) and 6(b) present the scatter plot of the perimeter and the length measured against those estimated (1 mm = 1 pixel). The results gave a correlation coefficient $(R^2) = 0.9779$, with RMSE of 14.37 mm, and $R^2 = 0.9609$ with RMSE of 7.143 mm for the perimeter and the length, respectively. This result concurs with those of Kronenberg et al. [45] who found a linear relationship, at $R^2 = 0.99$ between wheat stem length measured with terrestrial laser scanning and manually measured.

From Tables 3 and 4, the average relative error was 1.554% and 1.174% for the measured length and perimeter, respectively.

3.2. Statistical Analysis of Wheat Grain Yield Measured. Table 5 presents the descriptive statistics on the dataset. The statistical analysis of the 50 single wheat stem and their ear data of both varieties shows the mean values of 1.019 g and 1.060 g and a median of 0.949 g and 1.113 g and also a positive skew of 1.225 and 0.729 for the varieties "Luyuan 502" and "Zhengmai 9023", respectively. The positive skew of both varieties is indicating an asymmetrical distribution. The average and median of the measured parameter are higher than the mode according to the positive values of the skew.

3.3. Model Performance Evaluation. The developed models (Mdl 1, Mdl 2, Mdl 3, Mdl 4, Mdl 5, and Mdl 6) were evaluated on the test dataset for the two selected varieties (V502 and V9023). Table 6 shows the performance of the six models, and Table 7 summarizes the performance of these models. The results showed that, generally, the models were accurate in terms of grain yield prediction.

Linear regression outperformed all the explored models in the Mdl1, Mdl2, and for V502 in Mdl3 with the best prediction ($R^2 = 0.9893$) being for Mdl1 (V502). These results concur with the reports by Guérif et al. [46] that wheat grain yield could be estimated from the biomass index such as total dry matter, global incident solar radiation, photosynthetically active energy content, and the efficiency of interception of radiation by plant cover. Additionally, Dağüstü [47] and Kun et al. [15] established that the grain yield could be predicted using the weight and morphological parameters of the stem and the ear of wheat, respectively. Furthermore, Siddique et al. [48] reported that there exists an allometric relationship between the dry matter of the ear and the stem on one hand and, on the other hand, a positive correlation between the ear-stem ratio and the harvest index.

Using the wheat organ morphological features extracted from image processing to predict the grain yield, it can be seen that the Mdl5 gave the highest R^2 of 0.9665 and 0.9032 for V502 and V9032, respectively. Despite this accuracy being a little lower than that for Mdl1, it is still acceptable to use image morphological features of the wheat ear to predict the grain yield based on the results of previous studies such as Changying [49], who reported that the wheat grain yield and its ear image features are significantly correlated with the confidence of 95% and correlative coefficient of 0.9807. Also, Paulus et al. [50] proposed a 3D laser scanning method of wheat plants to estimate the volume of the wheat ears and to estimate the grain yield. Their technique achieved a precision of 96% in wheat ear segmentation and an R^2 of

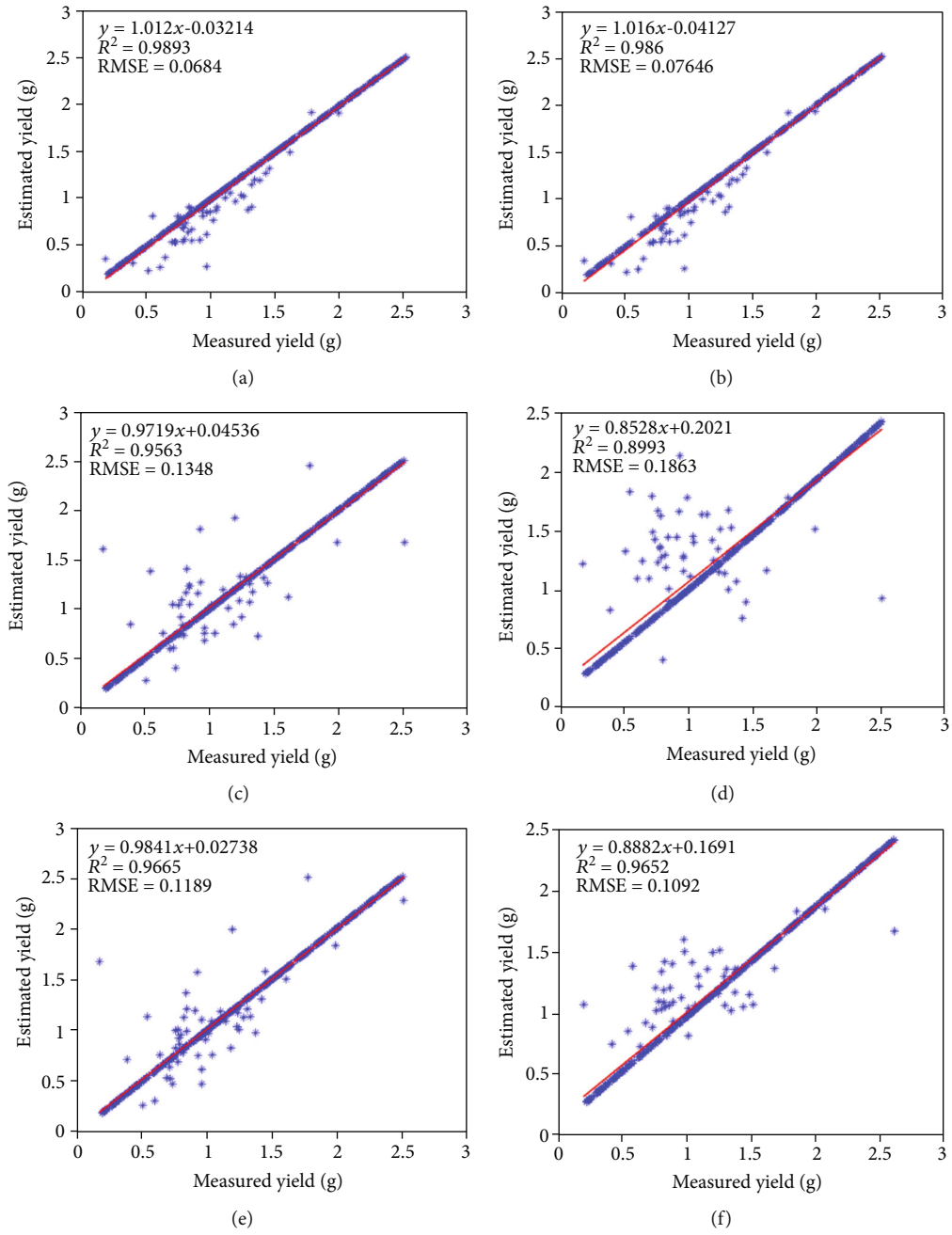

Figure 7: Scatter plot of the relationship between predicted and measured grain yield of the variety "Luyuan 502" for the six models: (a) Mdl1; (b) Mdl2; (c) Mdl3; (d) Mdl4; (e) Mdl5; and (f) Mdl6.

0.71 and 0.66 in correlation with the wheat ear volume to ear weight and yield, respectively.

Among the SVR models, the linear SVR gave the best prediction for Mdl4 (V9023) and Mdl6 (V502) at an R^2 of 0.9319 and 0.9652, respectively. Quadratic SVR outperformed all the other models in Mdl3 (V9023), Mdl4 (V502), Mdl5 (V9023), and Mdl6 (V9023) at R^2 of 0.931, 0.8993, 0.9032, and 0.9492, respectively. However, the cubic SVM and RBF SVR did not outperform any explored models in this study. Furthermore, cubic SVR returned the lowest accuracy in the entire testing dataset in comparison to other models. It can be explained by the fact that the Gaussian based SVR models have a good generalization ability and robustness on the testing dataset compared to polynomial SVRs; hence, the low accuracy in cubic SVR for model Mdl3, Mdl6 [42].

A variation can be observed between the dry yield estimation of V502 and V9023. This can be attributed to the analysis of a single set of data. Therefore, more than two cultivars and environmental conditions should be taken into account to determine the cause of the different variations for different wheat varieties.

Figures 7 and 8 depict the relationship between the measured and the estimated yield for all the best models for the varieties "Luyuan 502" and "Zhengmai 9023", respectively.

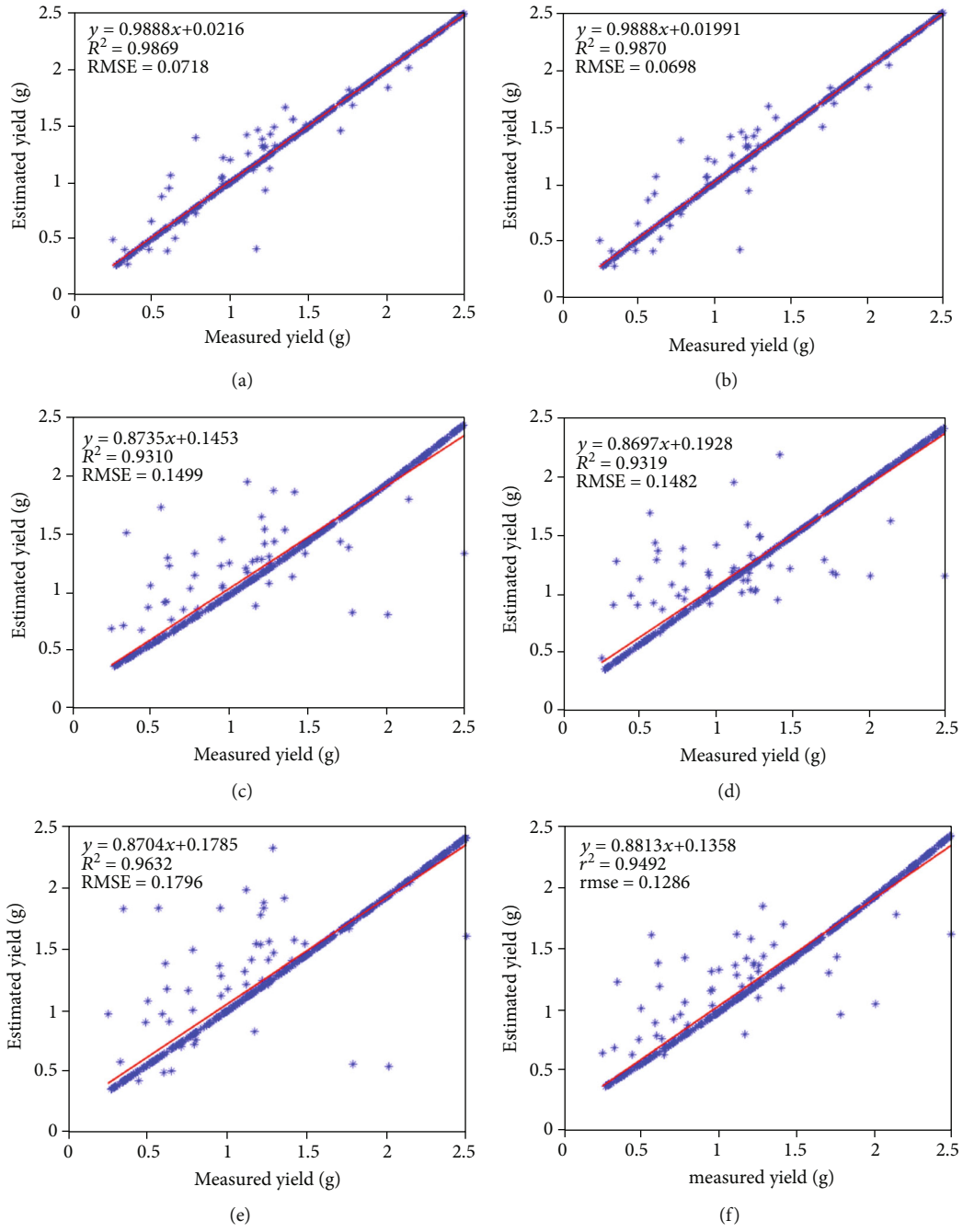

Figure 8: Scatter plot of the relationship between predicted and measured grain yield of the variety "Zhengmai 9023" for the six models: (a) Mdl1, (b) Mdl2, (c) Mdl3, (d) Mdl4, (e) Mdl5, and (f) Mdl6.

The field crop system is an open and complex system, which requires an exploration of the mechanisms of crop growth with reference to the complexity and precise regulation of crop groups [51]. Therefore, the analysis of the quality of the crop population requires a quantitative representation of individual phenotypic indicators in the population. The usual competition among plants in the population will lead to differences in the individual phenotypic indicators of the crops, which will affect the quality of the cultivated population and the final yield [52]. However, the physiological and ecological processes of crops in group conditions are still not accurately interpreted. As a result, phenotypic information on crops should be analyzed at the organ, plant, and population levels [53]. Based on an individual organ analysis, this study proposed a method for obtaining phenotypic biomass indicators, namely, the morphological parameters of a single stem and the ear of wheat, which provides a reference method and technology for interpreting the relationship between plants and assessing the quality of the population and for better understanding the effect of the interaction between genotypes and the environment (G × E) of crops on yield.

4. Conclusion

Breeders first identify phenotypes of interest to collect essential data for the characterization of the genetic material to improve plant productivity by hybridization genetically. Currently, various techniques and methodologies have been developed for the screening of biotic, abiotic, physiological, and biochemical traits in cultivated plants. In this study, image processing technology was applied to extract the morphological parameters (length, width, and perimeter) from wheat ears and stem and dry and wet matter weight to predict the final grain yield of wheat. The parameters derived from this technique can also be used in crop simulation models to simulate other phenotypes, such as plant disease detection, drought and water stress effects, and fertilization effects in plants. However, this study was based on only the effect of the stem and the ear morphology and the dry weight matter on the final yield. A future field study considering the morphological parameters of the stem and ear leaves at different growth stages would provide much more information on the morphological factors involved in the establishment of the final grain yield of wheat.

Data Availability

The data used to support the findings of the study can be available upon request to the corresponding author.

Conflicts of Interest

All the authors declare no conflict of interest.

Acknowledgments

Financial supports from the Jiangsu Agriculture Science and Technology Innovation Fund (CX(17)1002), State Key Program of China (2016YFD0300900), and Jiangsu Agri. Mech. Fund (201- 051028) were acknowledged.

References

[1] D. K. Ray, N. Ramankutty, N. D. Mueller, P. C. West, and J. A. Foley, "Recent patterns of crop yield growth and stagnation," *Nature Communications*, vol. 3, no. 1, pp. 1–7, 2012.

[2] S. Hafner, "Trends in maize, rice, and wheat yields for 188 nations over the past 40 years: a prevalence of linear growth," *Agriculture, Ecosystems and Environment*, vol. 97, no. 1-3, pp. 275–283, 2003.

[3] G. Bai, Y. Ge, W. Hussain, P. S. Baenziger, and G. Graef, "A multi-sensor system for high throughput field phenotyping in soybean and wheat breeding," *Computers and Electronics in Agriculture*, vol. 128, pp. 181–192, 2016.

[4] J. Crain, S. Mondal, J. Rutkoski, R. P. Singh, and J. Poland, "Combining high-throughput phenotyping and genomic information to increase prediction and selection accuracy in wheat breeding," *Plant Genome*, vol. 11, no. 1, pp. 1–14, 2018.

[5] J. S. Beckmann and M. Soller, "Restriction fragment length polymorphisms and genetic improvement of agricultural species," *Euphytica*, vol. 35, no. 1, pp. 111–124, 1986.

[6] J. Poland, J. Endelman, J. Dawson et al., "Genomic selection in wheat breeding using genotyping-by-sequencing," *Plant Genome*, vol. 5, no. 3, pp. 103–113, 2012.

[7] J. N. Cobb, G. DeClerck, A. Greenberg, R. Clark, and S. McCouch, "Next-generation phenotyping: requirements and strategies for enhancing our understanding of genotype–phenotype relationships and its relevance to crop improvement," *Theoretical and Applied Genetics*, vol. 126, no. 4, pp. 867–887, 2013.

[8] J. L. Araus, S. C. Kefauver, M. Zaman-Allah, M. S. Olsen, and J. E. Cairns, "Translating high-throughput phenotyping into genetic gain," *Trends in Plant Science*, vol. 23, no. 5, pp. 451–466, 2018.

[9] R. T. Furbank and M. Tester, "Phenomics–technologies to relieve the phenotyping bottleneck," *Trends in Plant Science*, vol. 16, no. 12, pp. 635–644, 2011.

[10] S. Dhondt, N. Wuyts, and D. Inzé, "Cell to whole-plant phenotyping: the best is yet to come," *Trends in Plant Science*, vol. 18, no. 8, pp. 428–439, 2013.

[11] M. Hussain, S. Farooq, K. Jabran, M. Ijaz, A. Sattar, and W. Hassan, "Wheat sown with narrow spacing results in higher yield and water use efficiency under deficit supplemental irrigation at the vegetative and reproductive stage," *Agronomy*, vol. 6, no. 2, p. 22, 2016.

[12] J. Mathan, J. Bhattacharya, and A. Ranjan, "Enhancing crop yield by optimizing plant developmental features," *Development*, vol. 143, no. 18, pp. 3283–3294, 2016.

[13] K. Watanabe, W. Guo, K. Arai et al., "High-throughput phenotyping of sorghum plant height using an unmanned aerial vehicle and its application to genomic prediction modeling," *Frontiers in Plant Science*, vol. 8, p. 421, 2017.

[14] P. Hu, S. C. Chapman, X. Wang et al., "Estimation of plant height using a high throughput phenotyping platform based on unmanned aerial vehicle and self-calibration: example for sorghum breeding," *European Journal of Agronomy*, vol. 95, pp. 24–32, 2018.

[15] B. Kun, J. Pan, L. Lei, S. Benyi, and W. Cheng, "Non-destructive measurement of wheat spike characteristics based on morphological image processing," *Transactions of the Chinese Society of Agricultural Engineering*, vol. 26, no. 12, pp. 212–216, 2010.

[16] J. Barker III, N. Zhang, J. Sharon et al., "Development of a field-based high-throughput mobile phenotyping platform," *Computers and Electronics in Agriculture*, vol. 122, pp. 74–85, 2016.

[17] J. M. Montes, F. Technow, B. S. Dhillon, F. Mauch, and A. E. Melchinger, "High-throughput non-destructive biomass determination during early plant development in maize under field conditions," *Field Crops Research*, vol. 121, no. 2, pp. 268–273, 2011.

[18] F. Hosoi and K. Omasa, "Estimating vertical plant area density profile and growth parameters of a wheat canopy at different growth stages using three-dimensional portable lidar imaging," *ISPRS Journal of Photogrammetry and Remote Sensing*, vol. 64, no. 2, pp. 151–158, 2009.

[19] N. Alharbi, J. Zhou, and W. Wang, "Automatic counting of wheat spikes from wheat growth images," in *Proceedings of the 7th International Conference on Pattern Recognition Applications and Methods*, pp. 346–355, Funchal, Madeira, Portugal, 2018.

[20] C. Germain, R. Rousseaud, and G. Grenier, "Non destructive counting of wheatear with picture analysis," in *Fifth*

International Conference on Image Processing and its Applications, Edinburgh, UK, July 1995.

[21] Y. Zhu, Z. Cao, H. Lu, Y. Li, and Y. Xiao, "In-field automatic observation of wheat heading stage using computer vision," *Biosystems Engineering*, vol. 143, pp. 28–41, 2016.

[22] L. Li, Q. Zhang, and D. Huang, "A review of imaging techniques for plant phenotyping," *Sensors*, vol. 14, no. 11, pp. 20078–20111, 2014.

[23] Z. Yu, X. Wang, and C. Feng, "Study on relationship between characters of haulm and characters on position of ear of wheat," *Journal of Hubei Agricultural College*, vol. 18, pp. 8–11, 1998.

[24] Z. Yang, N. Li, J. Ma, Y. Sun, and H. Xu, "High-yielding traits of heavy panicle varieties under triangle planting geometry: a new plant spatial configuration for hybrid rice in China," *Field Crops Research*, vol. 168, pp. 135–147, 2014.

[25] J. Zhang, Q. Ding, W. Ding et al., "Effect of stratified rotary tillage on paddy soil physical properties," *Journal of Nanjing Agricultural University*, vol. 38, pp. 1016–1022, 2015.

[26] J. C. Flinn and B. B. Khokhar, "Temporal determinants of the productivity of rice-wheat cropping systems," *Agricultural Systems*, vol. 30, no. 3, pp. 217–233, 1989.

[27] R. K. Lu, *Analysis methods of soil agricultural chemistry*, vol. 107, China Agricultural Science and Technology Press, Beijing, 2000.

[28] S. Ozpinar and A. Ozpinar, "Tillage effects on soil properties and maize productivity in western Turkey," *Archives of Agronomy and Soil Science*, vol. 61, no. 7, pp. 1029–1040, 2014.

[29] I. Etikan and K. Bala, "Sampling and sampling methods," *Biometrics & Biostatistics International Journal*, vol. 5, no. 6, p. 149, 2017.

[30] F. Yates and I. Zacopanay, "The estimation of the efficiency of sampling, with special reference to sampling for yield in cereal experiments," *The Journal of Agricultural Science*, vol. 25, no. 4, pp. 545–577, 1935.

[31] J. Svensgaard, T. Roitsch, and S. Christensen, "Development of a mobile multispectral imaging platform for precise field phenotyping," *Agronomy*, vol. 4, no. 3, pp. 322–336, 2014.

[32] Z. Zhang, "A flexible new technique for camera calibration," *IEEE Transactions on Pattern Analysis and Machine Intelligence*, vol. 22, no. 11, pp. 1330–1334, 2000.

[33] R. B. Austin, J. Bingham, R. D. Blackwell et al., "Genetic improvements in winter wheat yields since 1900 and associated physiological changes," *The Journal of Agricultural Science*, vol. 94, no. 3, pp. 675–689, 1980.

[34] S. Mukhopadhyay and B. Chanda, "Multiscale morphological segmentation of gray-scale images," *IEEE Transactions on Image Processing*, vol. 12, no. 5, pp. 533–549, 2003.

[35] L. Zheng, J. Zhang, and Q. Wang, "Mean-shift-based color segmentation of images containing green vegetation," *Computers and Electronics in Agriculture*, vol. 65, no. 1, pp. 93–98, 2009.

[36] G. Pajares, I. García-Santillán, Y. Campos et al., "Machine-vision systems selection for agricultural vehicles: a guide," *Journal of Imaging*, vol. 2, no. 4, p. 34, 2016.

[37] G. Deng and L. W. Cahill, "An adaptive Gaussian filter for noise reduction and edge detection," in *1993 IEEE Conference Record Nuclear Science Symposium and Medical Imaging Conference*, pp. 1615–1619, San Francisco, CA, USA, October-November 1993.

[38] N. Bairwa and N. Kumar Agrawal, "Development of counting algorithm for overlapped agricultural products," *International Journal of Computer Applications*, 2014.

[39] A. Khoshroo, A. Arefi, A. Masoumiasl, and G.-H. Jowkar, "Classification of wheat cultivars using image processing and artificial neural networks," *Agricultural Communications*, vol. 2, pp. 17–22, 2014.

[40] B. E. Boser, I. M. Guyon, and V. N. Vapnik, "A training algorithm for optimal margin classifiers," in *COLT '92: Proceedings of the fifth annual workshop on Computational learning theory*, New York, NY, USA, July 1992.

[41] I. Nyalala, C. Okinda, L. Nyalala et al., "Tomato volume and mass estimation using computer vision and machine learning algorithms: cherry tomato model," *Journal of Food Engineering*, vol. 263, pp. 288–298, 2019.

[42] C. Okinda, M. Lu, L. Liu et al., "A machine vision system for early detection and prediction of sick birds: a broiler chicken model," *Biosystems Engineering*, vol. 188, pp. 229–242, 2019.

[43] D. Li, W. Yang, and S. Wang, "Classification of foreign fibers in cotton lint using machine vision and multi-class support vector machine," *Computers and Electronics in Agriculture*, vol. 74, no. 2, pp. 274–279, 2010.

[44] Q. Wu and D.-X. Zhou, "Analysis of support vector machine classification," *Journal of Computational Analysis and Applications*, vol. 8, 2006.

[45] L. Kronenberg, K. Yu, A. Walter, and A. Hund, "Monitoring the dynamics of wheat stem elongation: genotypes differ at critical stages," *Euphytica*, vol. 213, no. 7, p. 157, 2017.

[46] M. Guérif, R. Delécolle, X. Gu, J. P. Guinot, M. Jappiot, and S. Steinmetz, "Estimation de la biomasse et du rendement de cultures de blé dur à partir des indices de végétation SPOT," *Proceedings of the Spectral Signatures of Objects in Remote Sensing*, vol. 287, p. 137, 1988.

[47] N. Dağüstü, "Genetic analysis of grain yield per spike and some agronomic traits in diallel crosses of bread wheat (Triticum aestivum L.)," *Turkish Journal of Agriculture and Forestry*, vol. 32, pp. 249–258, 2008.

[48] K. H. M. Siddique, E. J. M. Kirby, and M. W. Perry, "Ear: stem ratio in old and modern wheat varieties; relationship with improvement in number of grains per ear and yield," *Field Crops Research*, vol. 21, no. 1, pp. 59–78, 1989.

[49] G. H. J. Changying, "Estimating yield of wheat spike with its texture features based on image processing technology," *Transactions of the Chinese Society for Agricultural Machinery*, vol. 12, 2007.

[50] S. Paulus, J. Dupuis, A.-K. Mahlein, and H. Kuhlmann, "Surface feature based classification of plant organs from 3D laserscanned point clouds for plant phenotyping," *BMC Bioinformatics*, vol. 14, no. 1, p. 238, 2013.

[51] J. P. Walters, D. W. Archer, G. F. Sassenrath et al., "Exploring agricultural production systems and their fundamental components with system dynamics modelling," *Ecological Modelling*, vol. 333, pp. 51–65, 2016.

[52] X. Zhang, C. Huang, D. Wu et al., "High-throughput phenotyping and QTL mapping reveals the genetic architecture of maize plant growth," *Plant Physiology*, vol. 173, no. 3, pp. 1554–1564, 2017.

[53] M. Zhao, J. Qin, S. Li et al., "An automatic counting method of maize ear grain based on image processing," in *Computer and Computing Technologies in Agriculture VIII. CCTA 2014. IFIP Advances in Information and Communication Technology, vol 452*, D. Li and Y. Chen, Eds., pp. 521–533, Springer, Cham, 2014.